climate

Article

Comparative Trend Analysis of Precipitation Indices in Several Towns of the Sirba River Catchment (Burkina Faso) from CHIRPS and TAMSAT Rainfall Estimates

Giorgio Cannella *, Alessandro Pezzoli and Maurizio Tiepolo

Interuniversity Department of Regional and Urban Studies and Planning, Politecnico di Torino, Viale G. Mattioli 39, 10125 Torino, Italy; alessandro.pezzoli@polito.it (A.P.); maurizio.tiepolo@polito.it (M.T.)
* Correspondence: giorgio.cannella@polito.it

Abstract: The increasingly frequent pluvial flood of West African urban settlements indicates the need to investigate the drivers of local rainfall changes. However, meteorological stations are few, unevenly distributed, and work irregularly. Daily satellite rainfall datasets can be used. Nevertheless, these products often need to be more accurate due to sensor errors and limitations in retrieval algorithms. The problem is, therefore, how to characterize rainfall where there is a need for ground-based rainfall records or incomplete series. This study aims to characterize urban rainfall using two satellite datasets. The analysis was carried out in the Sirba river catchment, Burkina Faso, using the Climate Hazards Group InfraRed Precipitation with Station data (CHIRPS) and the Tropical Applications of Meteorology using SATellite and ground-based data (TAMSAT) datasets. Ten indices from the Expert Team on Climate Change Detection and Indices (ETCCDI) of precipitation were calculated, and their statistical trends were evaluated from 1983 to 2023. The study introduces two key innovations: a comparative analysis of precipitation trends using two satellite datasets and applying this analysis to towns within a previously understudied 39,138 km^2 catchment area that is frequently flooded. Both datasets agree on the increase of (i) annual cumulative rainfall over all towns, (ii) five-day maximum rainfall over the town of Manni, (iii) rainfall due to very wet days in Gayéri, (iv) days of heavy rainfall in Bogandé, Manni and Yalgho, and (v) days of very heavy rainfall in Yalgho. These findings suggest the need for targeted pluvial flood prevention measures in towns with increasing trends in heavy rainfall.

Keywords: rainfall regime; extreme indices; satellite precipitation products; trend analysis; flood risk analysis; urban Sahel

check for updates

Citation: Cannella, G.; Pezzoli, A.; Tiepolo, M. Comparative Trend Analysis of Precipitation Indices in Several Towns of the Sirba River Catchment (Burkina Faso) from CHIRPS and TAMSAT Rainfall Estimates. *Climate* **2024**, *12*, 208. https://doi.org/10.3390/cli12120208

Academic Editor: Charles Jones

Received: 24 October 2024
Revised: 22 November 2024
Accepted: 3 December 2024
Published: 4 December 2024

1. Introduction

West African towns are expanding rapidly due to significant population pressure [1]. This expansion needs to have appropriate stormwater drainage [2]. Consequently, the intensification of rainfall in urban settlements can increase the risk of pluvial flooding [3]. Understanding where and to what extent rainfall varies is crucial for reducing flood risk and proper water resource management in the region.

One of the most widely used methods to assess precipitation changes is the computation of precipitation indices [4]. These indices measure the intensity, frequency, and duration of daily or sub-daily precipitation on monthly, seasonal, or annual time scales. The Expert Team on Climate Change Detection and Indices (ETCCDI) has developed indices [5] that have become the standard for global [6], regional, and local climatology studies [7,8]. However, analyzing temporal and spatial variations in precipitation requires a long and homogeneous series of measurements. Without these conditions, Satellite Precipitation Products (SPPs) can be used [9–11]. However, SPPs have sensor errors, retrieval scheme errors due to the information processing algorithm, and product errors caused by the restitution of the surveys in daily or monthly time aggregates [12,13]. Furthermore, SPPs perform better in tropical areas than in semi-arid and mountainous regions [14] due to the variability in topography and localized climate conditions that affect the accuracy of satellite measurements [15,16]. The lack of precipitation data from the stations to correct satellite estimations influences the performance of SPPs [17].

West Africa is one of the areas least covered by station-based precipitation records. Many rainfall studies in this region have used alternative datasets, particularly the Climate Hazards Group Infrared Precipitation with Station (CHIRPS) satellite dataset [18–22]. However, comparing different SPPs in West Africa at the regional scale reveals that daily accuracy statistics perform worse than those at the monthly and annual scales [16,23–25].

Therefore, the problem is investigating changes in daily precipitation that affect West African towns without stations or whose precipitation records are not complete. This raises two research questions. First, what is the performance of SPPs in the long-term detection of urban precipitation at the daily scale? Second, can comparing trends obtained from two datasets raise confidence if they agree on specific precipitation characteristics? These questions are critical for improving the accuracy and reliability of rainfall data in urban contexts prone to pluvial flooding.

This study aims to characterize urban precipitations in semi-arid West Africa by comparing trends of climate indices derived from multiple datasets. Previously used globally [26] and in East Africa [27], this methodology is expected to work better than a single dataset for urban settlements in characterizing their rainfall trends.

The first novelty of the study is applying this methodology to urban-scale precipitation trends obtained from two satellite datasets. By comparing the CHIRPS and TAMSAT datasets, this study addresses the known limitations of individual satellite-based products. Cross-validation between these datasets mitigates potential biases in precipitation estimation, thus providing a more robust characterization of rainfall patterns over urban settlements.

The second novelty concerns the study area, which has yet to be investigated despite increasing pluvial flooding. The catchment is the Yali, Faga, and Koulouko rivers (39,138 km^2) in Burkina Faso. The three rivers join to form the Sirba River, which flows 120 km downstream into the Niger River. In the catchment, there are eight towns with more than 10,000 inhabitants, three of which have been hit by catastrophic pluvial floods in recent years [28]. The eight municipalities were, therefore, chosen as case studies because of their greater exposure to flood risk. Of these towns, however, three have no station, while four have gaps in their rainfall records from stations that do not allow the correct detection of rainfall trends. Nevertheless, the Bogandé station, with only 0.6% missing data over 40 years, enabled a comprehensive analysis of rainfall patterns and provided a ground-truth reference for evaluating the satellite datasets' performance. This study contributes to a more localized understanding of pluvial flood risk within the catchment area by applying advanced satellite-based trend analysis to this critical region.

In the following sections, the paper (i) presents the study area, (ii) describes the satellite products and the analysis methodology used, (iii) calculates the trends obtained from the two datasets and compares them, and (iv) discusses the results obtained concerning the scientific knowledge on this topic.

2. Materials and Methods

2.1. Study Area

According to the Koppen Geiger classification, the Sirba River catchment covers 39,138 km^2 in the Bsh-hot semi-arid climate zone [29]. Of this catchment, 93% is in Burkina Faso and 7% in Niger. The Yali, Faga, and Koulouko rivers flow into the Sirba River, almost at the border between the two states, which in turn flows into the Niger River 120 km further downstream (Figure 1). The catchment is characterized by an elevation change of 272 m between the highest (461 m) and lowest (189 m) elevation. The land cover is mainly a mosaic of uncultivated savannahs, rain-fed crops, especially millet, and sparse tree cover. The catchment is exposed to a long dry season and short wet season, the latter occurring between June and September, accumulating rainfall levels between 400 and 700 mm/year [30]. However, long dry spells and extreme rainfall characterize the regime [31]. According to the last population census (2022), there are eight towns in the catchment with more than 10,000 inhabitants: Arbinda (45,818), Bogandé (21,443), Boulsa (24,200), Gayéri (15,170), Manni (15,066), Pissila (23,420), Sebba (11,298), and Yalgho (26,340) [32,33] (Table 1). These towns were selected due to their vulnerability to recent pluvial floods, making them key areas for assessing trends in precipitation and associated risks [28].

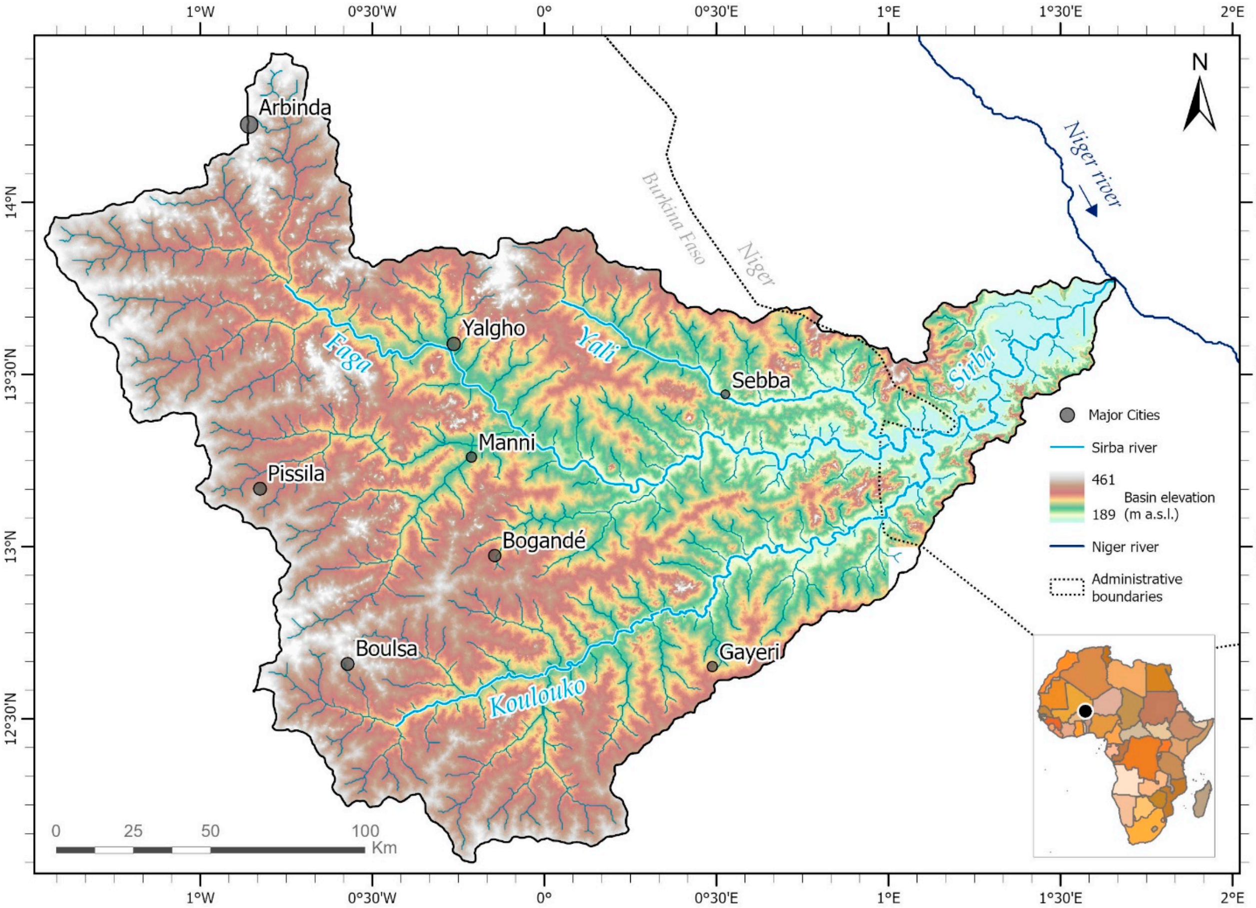

Figure 1. The Sirba River catchment.

Table 1. Towns in the Sirba river catchment (Burkina Faso).

City	Latitude	Longitude	Population 2022
Arbinda	14.22715	−0.8678992	45,818
Bogandé	12.97806	−0.140138	21,433
Boulsa	12.66383	−0.56815	24,200
Gayéri	12.65183	0.4885482	15,170
Manni	13.25976	−0.21249	15,066
Pissila	13.16794	−0.82718	23,420
Sebba	13.43504	0.521851	11,289
Yalgho	13.58896	−0.262852	26,340

2.2. Data Sources

Eleven weather stations in the catchment have been active for forty years. Three have numerous missing data (18–22%) (Table 2). This study used only the eight stations with less than 10% missing data to evaluate the performance of the two SPPs.

Table 2. Sirba River (Burkina Faso) rainfall stations, length of daily records, and percentage of missing data.

Station	Latitude	Longitude	Time Analysis	Data Missing (%)
Arbinda	14.22715	−0.8678992	March 1982–March 2022.	6.1
Bani	13.71752	−0.169166	October 1982–October 2022	15.6
Barsalogho	13.47110	−1.05768	January 1982–January 2022	0.1
Bogandé	12.97806	−0.140138	January 1982–January 2022	0.6
Boulsa	12.66383	−0.56815	January 1981–January 2021	4
Bouroum	13.61026	−0.64877	January 1982–January 2022	18
Dakiri	13.29182	−0.25508	January 1982–January 2022	1
Gayéri	12.65183	0.4885482	January 1982–January 2022	5
Kossougoudou	12.93667	−0.22866	January 1982–January 2022	19
Piéla	12.70381	−0.13211	January 1982–January 2022	2
Sebba	13.43503	0.52185	January 1982–January 2022	6

The global CHIRPS and regional TAMSAT datasets were first tested on selected stations and then used to analyze rainfall trends in the eight major towns on which the study focuses. From these SPPs, years of daily measurements (1983–2023) were extracted first at the coordinates of the eight selected stations to evaluate their performance statistically. Subsequently, the series of the three cities not covered by stations (Manni, Pissila, and Yalgho) were downloaded to analyze urban rainfall trends. This provided the study with eight complete daily precipitation datasets for evaluating changes in the eight towns of interest. The homogeneity of the data was assessed using the RClimdex software's 'quality control' function.

CHIRPS, produced by the Climate Hazards Center in collaboration with the U.S. Geological Survey, has been available since 2015 and provides daily, pentad, and monthly estimates of precipitation from 1981 to the present on a nearly global scale (50° S–50° N). The estimates are available at a resolution of 0.05° × 0.05° of latitude-longitude gridding. The dataset is realized through the use of CHPclim global climatology (0.05° × 0.05° scale), observations in the infrared band from geostationary satellites, ground stations (GHCN, GSOD), and atmospheric circulation and precipitation models (CFSv2)5 [34,35].

TAMSAT provides estimates of rainfall, climatology, and anomalies at the daily, pentad, decadal, monthly, and seasonal scales, at a resolution of 0.0375° × 0.0375° for Africa from January 1983 to the present. The dataset is constructed from infrared images recorded by the EUMETSAT satellites and rainfall time series recorded by African national meteorology and hydrology station stations [36,37].

The two datasets were selected based on results obtained in previous work evaluating the performance of SPPs in the region, whereby CHIRPS and TAMSAT were often found to be the two best performing. The performance of seven SPPs (ARC2, CHIRPS, PERSIANN, RFE, TARCAT, TRMM3B42, TRMM3B43) on the territory of Burkina Faso over the period 2001–2014 on the daily timescale was found to be unsatisfactory, with the best performance recorded by the CHIRPS dataset [23]. A comparison of seven SPPs (ARC2, CHIRPS, GPCP, PERSIANN, RFE, TAMSAT, TRMM) over the Sahelian climatic zone of Burkina Faso showed the TAMSAT and RFEv2 datasets as the best performing on the daily timescale [16].

The RClimdex quality control processes include checking for outliers, ensuring data consistency, and testing for homogeneity to confirm that the data series is suitable for long-term trend analysis. These steps ensure that the dataset is reliable for detecting precipitation trends over the study area. Considering the results obtained, the CHIRPS and TAMSAT datasets were selected for further analysis due to their higher performance at the daily timescale and the availability of a 40-year survey series (Figure 2).

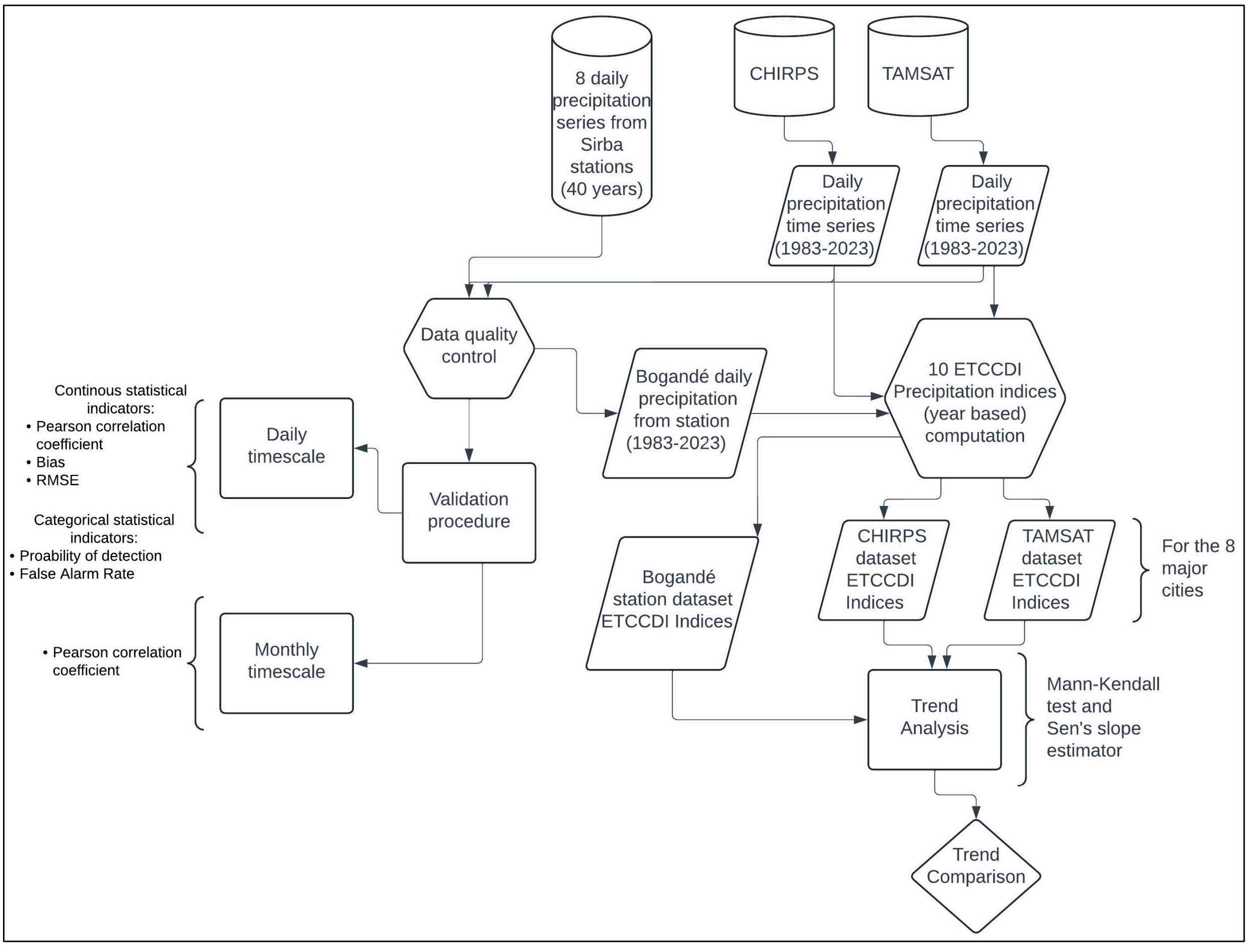

Figure 2. Flowchart of the analysis.

2.3. Satellite Datasets Validation Procedure

The two chosen SPPs were first validated on the station data available in correspondence with the catchment meteorological stations with less than 10% missing data. Each measurement point contains a time series of 40 years of daily precipitation data. The method of assessing the performance of the two models compares the daily precipitation values from the measurement point model with corresponding available values from the station based on statistical indicators (Table 3).

Table 3. Statistical validation indices of satellite datasets.

Statistical Indicator	Formula	Value Range	Ideal Value
Pearson correlation coefficient (r)	$r = \frac{\sum_{i=1}^{n}\left(G_i - \overline{G}\right)\left(S_i - \overline{S}\right)}{\sqrt{\sum_{i=1}^{n}\left(G_i - \overline{G}\right)^2}\sqrt{\sum_{i=1}^{n}\left(S_i - \overline{S}\right)^2}}$	−1 to 1	1
Bias	$\text{Bias} = \frac{\sum_{i=0}^{n} S_i}{\sum_{i=0}^{n} G_i}$	0 to ∞	1
Root Mean Square Error	$RMSE = \frac{\sqrt{\frac{1}{n}\sum_{i=0}^{N}\left(G_i - S_i\right)^2}}{\overline{G}_i}$	0 to ∞	0
Probability of Detection	POD = H/(H + M)	0 to 1	1
False Alarm Rate	FAR = F/(H + F)	0 to 1	0

CHIRPS and TAMSAT were selected for this study due to their superior performance in previous evaluations across Burkina Faso. These evaluations demonstrated better accuracy on a daily timescale than other Satellite Precipitation Products, making them ideal for long-term trend analysis in this region.

The performance evaluation of the two SPPs on a daily scale followed a point-by-point statistical comparison procedure, comparing the daily cumulative quantities from the satellite with those available from the stations (thus editing the daily satellite datasets by excluding days not detected by station). A set of statistical performance indices was calculated on the continuous data (Pearson correlation coefficient, Bias, Root Mean Square Error) and the categorical data through a contingency table (Probability of Detection, False Alarm Rate).

In a second step, the correlation (Pearson correlation coefficient) between the edited datasets and the station series on monthly mean values was also evaluated, following this procedure: (i) for each measurement point, the average values of the twelve months were processed; (ii) the correlation of these values was calculated based on the average twelve months values by station; (iii) the correlation values obtained for the twelve months were then averaged with each other to obtain a single correlation value that was representative for each measurement point.

2.4. ETCCDI Precipitation Index Analysis

Ten ETCCDI precipitation indices, processed using RClimdex software (Table 4), assessed changes in the precipitation regime annually. The indices were selected to emphasize changes in intensity (cumulative quantities, maximum and above a certain percentile threshold, rainy days above a certain amount) and duration of precipitation events (consecutive wet or dry days), as these metrics are critical for understanding both the frequency and severity of extreme precipitation events that contribute to urban flood risk.

Table 4. List of ETCCDI rainfall indices used in the analysis [5].

ID	Definition	Unit of Measurement
PRCPTOT	Total precipitation from days with cumulative rainfall $\geq$ 1 mm	mm
CDD	Maximum number of consecutive dry days (cumulative rainfall < 1 mm)	days
CWD	Maximum number of consecutive precipitating days	days
RX1day	Maximum one-day precipitation	mm
RX5day	Maximum five-day precipitation	mm
R10mm	Heavy precipitation days (with cumulative rainfall $\geq$ 10 mm)	days
R20mm	Very heavy precipitation days (with cumulative rainfall $\geq$ 20 mm)	days
R95p	Precipitation due to very wet days (<95th percentile)	mm
R99p	Precipitation due to extremely wet days (>99th percentile)	mm
SDII	Mean precipitation amount on a wet day	mm/day

These indices were calculated from the daily precipitation series for the eight towns in the catchment. Series, derived from the two SPPs, were downloaded at the coordinates of the weather stations. For the three towns without stations (Manni, Pissila, Yalgho), data were downloaded at the intersections of the two main roads (coordinates in Table 1).

For Bogandé station, which has the most complete record in the catchment, we compared ETCCDI indices calculated from ground measurements and satellite datasets.

2.5. Trend Analysis

The temporal trend of each index was evaluated using two statistical procedures: Sen's slope estimation and the Mann–Kendall significance test. Sen's slope estimation is used to estimate the slope and direction of the trend [38]. It is a non-parametric method of calculating the median slope, with positive values indicating increasing trends and negative values indicating decreasing trends. This method is ideal for identifying monotonic trends in non-normally distributed data, making it well-suited for analyzing precipitation variability. The Mann–Kendall test is also non-parametric and recommended by the World Meteorological Organisation for detecting trends in time series [39]. It provides information about the statistical significance of trends, which are considered significant when the p-value is less than 0.05. The significance threshold of $p < 0.05$ ensures that identified trends are statistically robust, helping distinguish between random variability and meaningful long-term changes in precipitation patterns.

These methods are particularly suitable for identifying monotonic trends in precipitation, especially in semi-arid regions like West Africa, where rainfall variability is high.

3. Results

The study investigated how to characterize rainfall changes that affect West African urban settlements without stations or whose precipitation series still need to be completed. This raises two research questions related to (i) the performance of SPPs in long-term urban rainfall observations and (ii) the comparison of trends obtained from two datasets as a method of raising confidence if they agree on specific rainfall characters.

3.1. Performance of Satellite-Based Precipitation Products

Five statistical accuracy indicators were used to examine the CHIRPS and TAMSAT daily rainfall datasets for 1983–2023. The indices obtained at the eight stations were then averaged to represent the individual model's performance over the catchment.

The CHIRPS dataset (Table 5) reported excellent Bias values (−0.02), slightly underestimating the station data. However, the correlation values, framed by Pearson's coefficient, were low (0.35). The low daily accuracy could be due to the coarse spatial resolution of the satellite datasets and limited ground station data for calibration. The index concerning the root mean square error (RMSE) identifies mean errors of 6.94 mm. Concerning the POD and FAR indices derived from the contingency table, the values obtained are almost equivalent (POD = 0.61 and FAR = 0.63), thus defining a certain degree of overestimating the frequency of precipitation events.

Table 5. Statistical accuracy performance of the CHIRPS model against station data.

	Arbinda	**Barsalogho**	**Bogandé**	**Boulsa**	**Dakiri**	**Gayéri**	**Piela**	**Sebba**	**Medium Value**
Pearson correlation	0.45	0.35	0.36	0.32	0.29	0.39	0.32	0.32	0.35
Bias	−0.04	−0.07	−0.19	0.05	0.13	−0.08	0.11	−0.07	−0.02
RMSE (mm)	5.66	6.91	6.91	7.66	6.88	7.24	7.24	6.99	6.94
POD	0.68	0.62	0.60	0.57	0.56	0.64	0.61	0.58	0.61
FAR	0.60	0.61	0.59	0.62	0.73	0.63	0.65	0.64	0.63

The TAMSAT dataset (Table 6) has higher correlation values (Pearson = 0.46) but slightly lower Bias values (−0.10), thus underestimating more than the other model (the lower the Bias values, the greater the underestimation of the measured data). The RMSE index frames a lower mean error than the other model (RMSE = 6.17 mm). As for the POD and FAR indices, derived from the contingency table, the values obtained frame a greater POD than FAR (POD = 0.83 and FAR = 0.64), again defining a certain degree of overestimation of the frequency of precipitation events but a more significant overall detection capacity.

Table 6. Statistical accuracy performance of the TAMSAT model against station data.

	Arbinda	**Barsalogho**	**Bogandé**	**Boulsa**	**Dakiri**	**Gayéri**	**Piela**	**Sebba**	**Medium Value**
Pearson correlation	0.34	0.53	0.57	0.40	0.43	0.48	0.48	0.48	0.46
Bias	−0.15	−0.13	−0.16	−0.07	−0.01	−0.14	−0.03	−0.12	−0.10
RMSE	5.90	5.99	5.78	6.90	6.02	6.53	6.18	6.08	6.17
POD	0.70	0.88	0.91	0.79	0.81	0.84	0.84	0.82	0.83
FAR	0.70	0.61	0.56	0.63	0.72	0.65	0.65	0.63	0.64

The Pearson correlation between average monthly values from stations and satellite datasets is 0.998 for CHIRPS and 0.997 for TAMSAT (Table 7).

Table 7. Correlation values (Pearson coefficient) between the station dataset and satellite dataset at a monthly scale.

	CHIRPS Dataset	TAMSAT Dataset
Arbinda	0.996	0.996
Barsalogho	0.997	0.997
Bogandé	0.998	0.994
Boulsa	0.999	0.997
Dakiri	0.998	0.999
Gayéri	0.998	0.999
Piela	0.998	0.997
Sebba	0.998	0.996
Mean All Stations	0.998	0.997

3.2. Comparison of Rainfall Trends

Precipitation indices trends were calculated using 40 years of daily precipitation measurements from the station for the town of Bogandé and 40 years of daily precipitation estimates from the CHIRPS and TAMSAT datasets over the eight towns in the catchment.

3.2.1. Bogandé Station Dataset

The following results evaluated statistical trends (Mann–Kendall test and Sen's slope analysis) on the indices extracted via the Bogandé station dataset (Table 8).

Table 8. Sen's slope values are processed on precipitation indices from the Bogandé station dataset. Values in blue identify increasing trends, and those in red are decreasing trends (the intensity of the color is proportional to the magnitude of the trend). Significant trends are bold: one star (*) identifies trends with a p-value < 0.05.

Bogandé Station	Sen's Slope Value
PRCPTOT	1.76
SDII	−0.03
CDD	0.35
CWD	**0 ***
RX1day	0.35
RX5day	**0.60 ***
R95P	1.91
R99P	0
R10mm	0
R20mm	0

The consecutive wet days (CWD) index is stationary and statistically significant. The five-day maximum rainfall index (RX5day) shows a statistically significant positive trend (+0.60 mm/year). Trends on the other indices do not show statistical significance. Of these, three were stationary (R99p, R10mm, R20mm), four were positive (PRCPTOT, CDD, RX1day, R95P), and one was slightly negative (SDII).

3.2.2. CHIRPS Dataset

The following results evaluated statistical trends (Mann–Kendall test and Sen's slope analysis) on the indices extracted via the CHIRPS model for the eight towns (Table 9).

Table 9. Sen's slope values are processed on precipitation indices from the CHIRPS dataset. Values in blue identify increasing trends, and those in red are decreasing trends (the intensity of the color is proportional to the magnitude of the trend). Significant trends are shown in bold: one star (*) identifies trends with a p-value < 0.05; two stars (**) identify a highly significant trend with a p-value < 0.01.

	Arbinda	Bogandé	Boulsa	Gayéri	Manni	Pissila	Sebba	Yalgho
PRCPTOT	**3.80 ** **	**2.76 ** **	**4.33 ** **	**3.95 ** **	**3.82 ** **	**3.71 ** **	**3.60 ** **	**3.80 ** **
SDII	0.04	0.01	0.03	0.03	**0.03 ***	**0.03 ***	0.02	0.03
CDD	−0.20	0.18	0.08	0.09	0.33	0.46	0.30	0.23
CWD	0	0	0	0	**−0.04 ***	0	0	**−0.03 ***
RX1day	0.14	−0.05	−0.08	0.09	0.11	−0.11	0.02	0.10
RX5day	0.01	0.21	0.19	0.26	**0.33 ***	0.11	0.10	0.27
R95P	1.02	0.30	0.44	**2.38 ** **	1.30	0.50	0.47	1.08
R99P	0	0	0	0	0	0	0	0
R10mm	**0.14 ***	**0.11 ** **	**0.23 ** **	**0.15 ** **	**0.19 ** **	**0.18 ** **	**0.12 ***	**0.14 ***
R20mm	0	0	0.08	0.05	**0.08 ***	**0.06 ***	0.04	**0.06 ***

The cumulative annual precipitation (PRCPTOT) is increasing in all locations, with an average positive trend of +3.7 mm/year and statistical significance of over 99% (p-value < 0.01). Days of heavy rainfall (R10mm) are increasing, with significant trends in all towns, averaging 1.5 more days per decade. The intense rain (R20mm) increased by an average of 2.5 more days over the 40-year survey period in Manni, Pissila, and Yalgho. The simple daily intensity (SDII) is statistically significant and slightly increasing (+0.03 mm/year) in Manni and Pissila. Consecutive wet days (CWD) have substantial and slightly decreasing trends only in Manni and Yalgho (−0.04 and −0.03 days/year, respectively). The maximum one-day rainfall (RX1day) shows a mix of positive and negative trends without statistical significance; the maximum five-day rainfall (RX5day) has a statistically significant increase (+0.33 mm/year) only in Manni. Precipitation due to very humid days (>95th percentile) (R95p) is substantial and positive only at Gayéri (+2.38 mm/year). Rainfall due to extremely humid days (>99th percentile) is stationary and non-significant in all towns. Consecutive dry days (CDD) are not statistically significant in any town.

3.2.3. TAMSAT Dataset

The evaluation of statistical trends (Mann–Kendall test and Sen's slope analysis) on the indices extracted through the TAMSAT model produced the following results (Table 10).

The cumulative precipitation index (PRCPTOT) is increasing in all towns, with a positive trend averaging +2.7 mm/year and statistical significance above 99% (p-value < 0.01). The maximum one-day precipitation (RX1day) shows positive trends with statistical significance in Sebba and Yalgho (+0.12 mm/year and +0.15 mm/year, respectively). The five-day maximum rainfall (RX5day) is increasing with significant trends in four towns (Bogandé, Manni, Sebba, Yalgho), with an average increase of +2.76 mm/decade. Precipitation due to very humid days (>95th percentile) (R95p) shows positive and significant trends in the towns of Bogandé, Gayéri, Manni, and Pissila, with an average increase of +1.35 mm/year. Precipitation due to extremely humid days (>99th percentile) (R99p), on the other hand, is slightly increasing in the city of Yalgho alone (+0.8 mm/decade). The days of heavy rainfall (R10mm) are rising with significant trends in Bogandé, Manni, and Yalgho (average increase of +1 day/decade); the index concerning the days of very heavy rainfall (R20mm) instead shows two significant trends: a stationary trend in Sebba (±0 days/year) and a slightly positive trend in Yalgho (+0.06 days/year). The simple daily intensity (SDII) shows a significant trend in Arbinda with a slightly negative trend (−0.01 mm/year). Consecutive dry days (CDD) decrease statistically significantly in four towns (Arbinda, Boulsa, Manni, Pissila) with an average of about −9 days/decade. Finally, the index of consecutive wet days (CWD) does not show statistical significance in any analyzed town.

Table 10. Sen's slope values were processed on precipitation indices from the TAMSAT dataset. Values in blue identify increasing trends, and those in red are decreasing trends (the intensity of the color is proportional to the magnitude of the trend). Significant trends are shown in bold: an asterisk (*) identifies trends with p-value < 0.05; two asterisks (**) identify a highly significant trend with p-value < 0.01.

	Arbinda	Bogandé	Boulsa	Gayéri	Manni	Pissila	Sebba	Yalgho
PRCPTOT	**1.89 ** **	**2.02 ** **	**2.21 ** **	**2.02 ** **	**1.78 ** **	**2.15 ** **	**2.50 ** **	**2.01 ** **
SDII	**−0.01 ** **	0	0	−0.01	0	0	0	−0.01
CDD	**−1.24 ** **	−0.36	**−0.55 ** **	−0.44	**−0.87 ** **	**−0.93 ** **	−0.65	−0.69
CWD	0	0	0	0.00	0	0.03	0	0
RX1day	0.07	0.05	0.02	0.04	0.11	0.09	**0.12 ***	**0.15 ***
RX5day	0.02	**0.33 ** **	0.17	0.18	**0.27 ** **	0.18	**0.22 ***	**0.27 ***
R95P	0.33	**1.13 ***	0.99	**2.06 ** **	**1.12 ***	**1.07 ***	0.95	0.79
R99P	0	0	0	0	0.08	0.09	0	**0.08 ***
R10mm	0	**0.11 ***	0.08	0.05	**0.10 ***	0.06	0.07	**0.14 ***
R20mm	0	0	0	0	0	0	**0 ***	**0.06 ***

3.2.4. Comparison of Trends Obtained from the Two SPPs Datasets

The trend analysis of the ten indices, conducted on the two datasets derived from the CHIRPS and TAMSAT models, produced different results depending on the product used.

The statistical significance of the trends was ascertained using the Mann–Kendall test. Consequently, it was possible to identify the elements of agreement between the two models, defined as those trends with equal direction and significance in both models. The two models agree on the following trends: (i) increasing total rainfall (with highly significant trends) over all towns, (ii) positive and statistically significant 5-day maximum rainfall for Manni (Figure 3a,b), (iii) statistically significant increasing rainfall due to very wet days in Gayeri (Figure 3c,d), (iv) days of heavy rainfall greater than 10 mm statistically significant increase in Bogandé, Manni, and Yalgho (Figure 3e,f), (v) days of very heavy rainfall greater than 20 mm slightly increasing and statistically significant in Yalgho (Figure 3g,h).

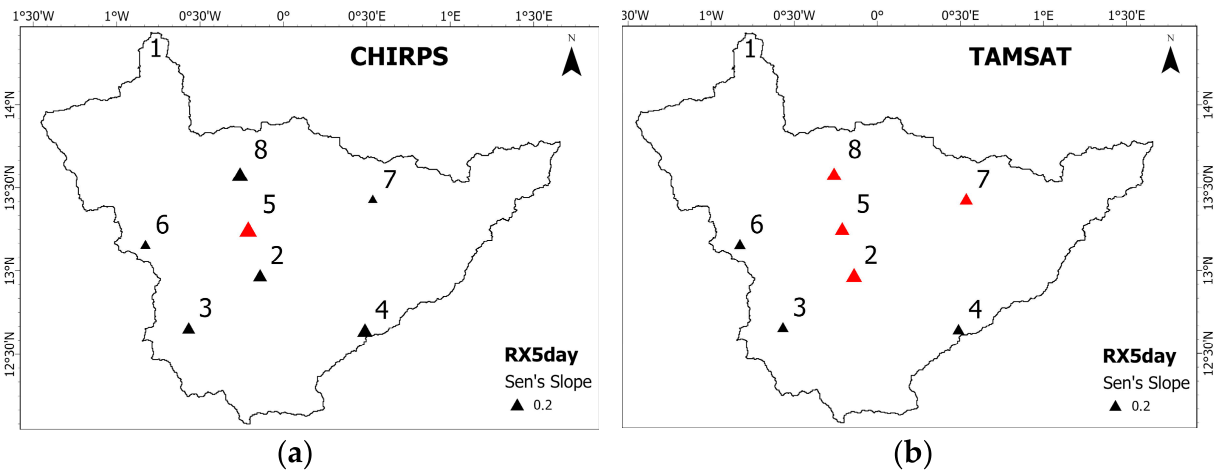

Figure 3. *Cont.*

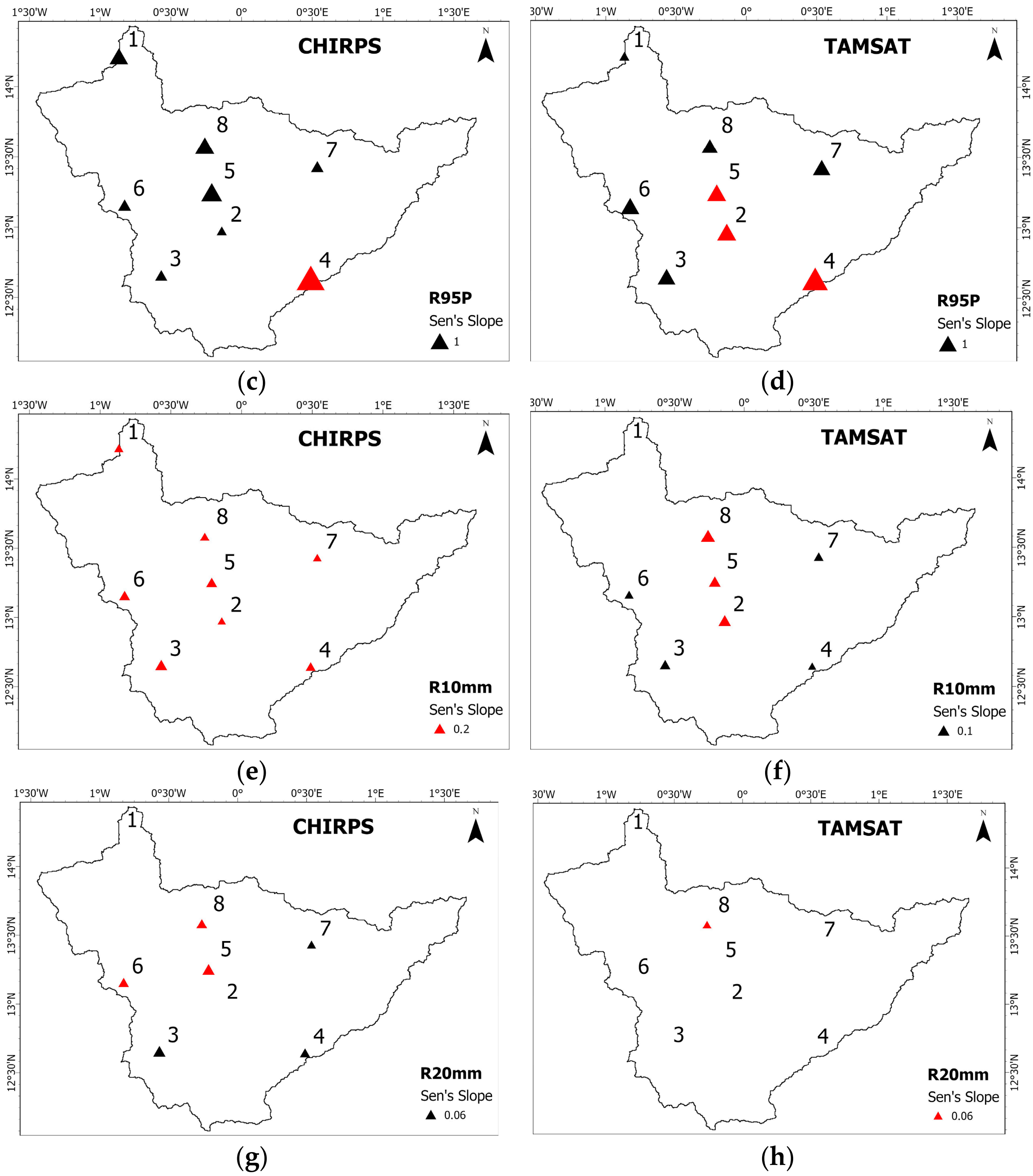

Figure 3. Trends for indices RX5 (**a**,**b**), R95P (**c**,**d**), R10mm (**e**,**f**), and R20mm (**g**,**h**) from CHIRPS and TAMSAT datasets. The size of the triangles is proportional to the magnitude of the trends. Red triangles identify trends with statistical significance. (1-Arbinda; 2-Bogandé; 3-Boulsa; 4-Gayéri; 5-Manni; 6-Pissila; 7-Sebba; 8-Yalgho).

The increase in cumulative annual precipitation at all towns and on both datasets shows a catchment-wide trend towards a wetter climate. The CHIRPS dataset detects this increase with greater magnitude.

On the other hand, the two datasets present divergent results, i.e., trends whose significance (ascertained by the Mann–Kendall test) or direction (evaluated by Sen's slope) is contradicted by one model over the other. These results concern: (i) the decrease in consecutive dry days statistically significant in four towns (Arbinda, Boulsa, Manni, Pissila) by TAMSAT, which is contradicted by the increasing trends by CHIRPS model for the same locations (but without statistical significance) (Figure 4a,b); (ii) slight decrease in consecutive wet days, statistically significant on CHIRPS for two towns (Manni and Yalgho), contradicted by the stationarity of the index via TAMSAT for the same locations (but without statistical significance) (Figure 4c,d); (iii) the slightly decreasing simple daily intensity index in Arbinda detected by TAMSAT is positive on CHIRPS. When analyzed by CHIRPS, the index presents positive and significant trends for Manni and Pissila, which are stationary on TAMSAT (Figure 4e,f); (iv) the slightly increasing precipitation due to extremely wet days detected in Yalgho by TAMSAT is stationary on CHIRPS (but without statistical significance).

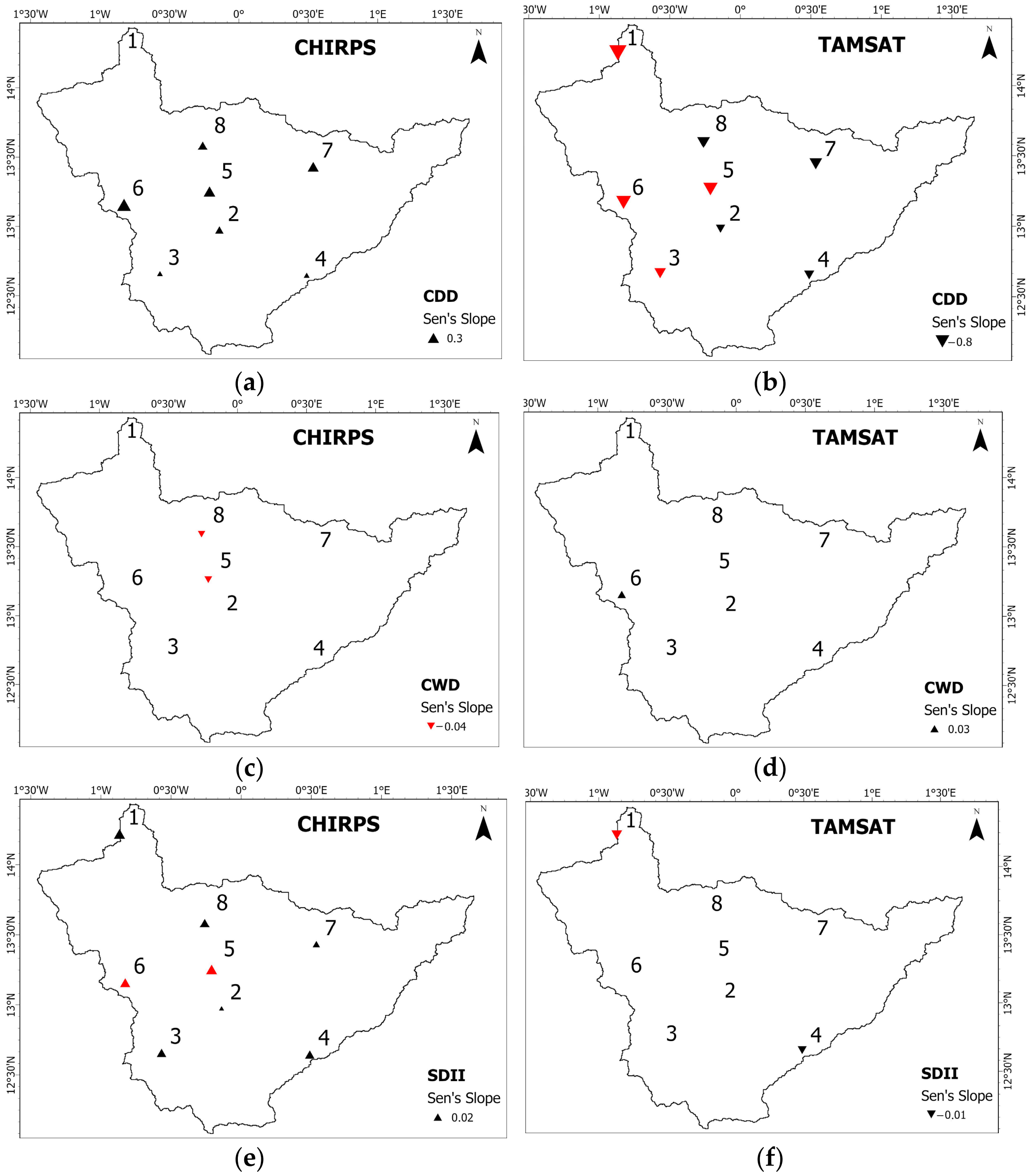

Figure 4. The trend for the CDD (**a**,**b**), CWD (**c**,**d**), and SDII (**e**,**f**) indices from CHIRPS and TAMSAT datasets. The orientation of the triangles is related to the direction of the trend (upward for positive trends, downward for negative trends). The size of the triangles is proportional to the magnitude of the trends. Red triangles identify trends with statistical significance. (1-Arbinda; 2-Bogandé; 3-Boulsa; 4-Gayéri; 5-Manni; 6-Pissila; 7-Sebba; 8-Yalgho).

To summarise, major differences concern indexes of consecutive dry and wet days. The first is increasing in the case of CHIRPS and decreasing in the case of TAMSAT. The latter shows a slight decrease in CHIRPS, contradicted by stationarity on TAMSAT. Furthermore, the simple daily intensity index shows a slightly positive trend in the CHIRPS dataset and a stationary or somewhat negative trend in the TAMSAT dataset. These inconsistencies may result from differences in the algorithms used by CHIRPS and TAMSAT, particularly in regions with sparse data coverage.

3.2.5. Comparison of Trends for the Town of Bogandé

For the town of Bogandé, trends for the ten ETCCDI indices were calculated on both the station and satellite datasets. This allows a comparison of the different results obtained for the same city, depending on the types of datasets used.

The significant trends obtained for the city of Bogandé identify (i) stable CWD and positive RX5day on the station dataset; (ii) PRCPTOT and R10mm increasing on the CHIRPS dataset; and (iii) PRCPTOT, R10mm, and RX5day increasing on the TAMSAT dataset (Figure 5).

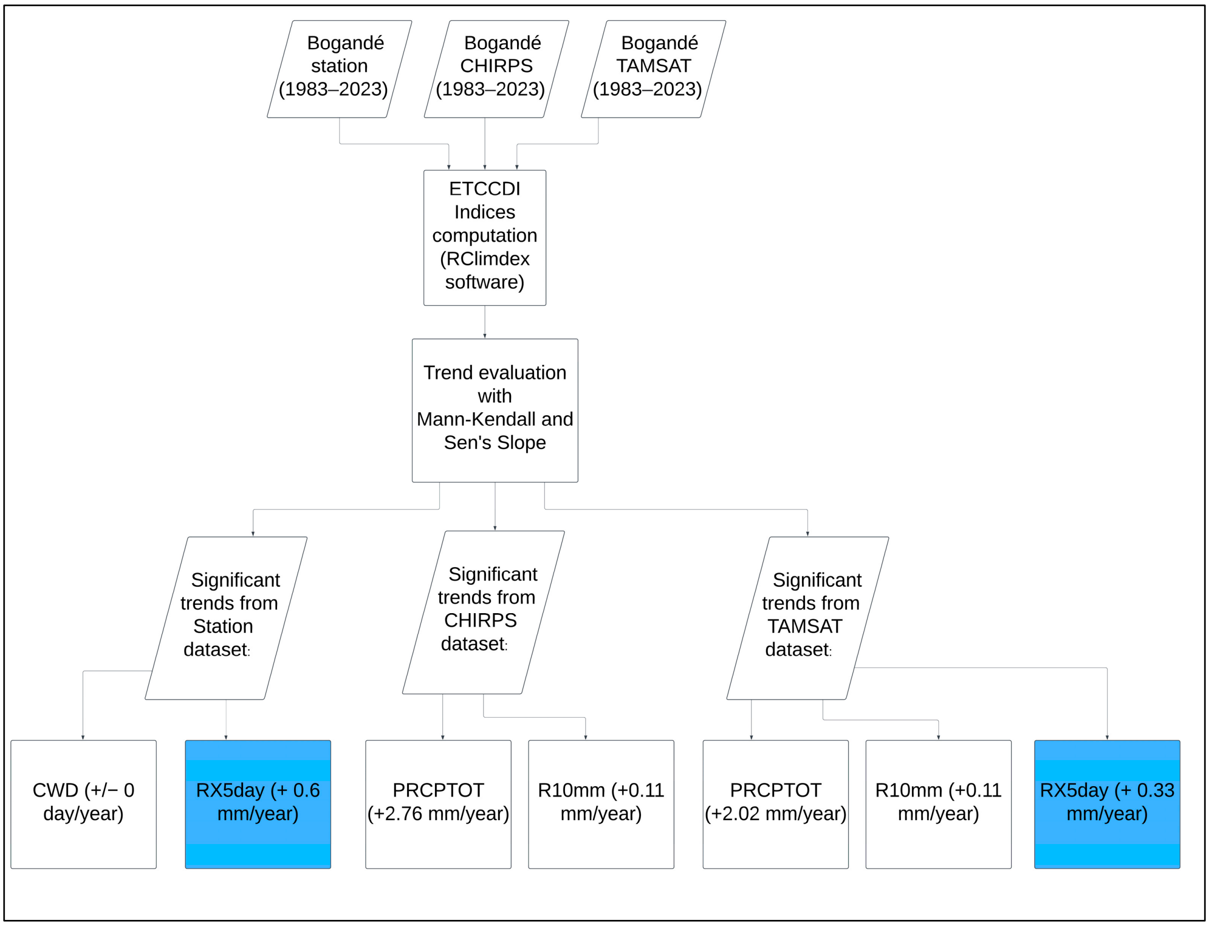

Figure 5. Flowchart and infographic of the comparison of rainfall trends at Bogandé. In blue are the elements of agreement between station and SPPs datasets.

The results agree regarding the RX5day parameter, whose increase is detected by both the station and TAMSAT datasets.

4. Discussion

This study aimed to address two key questions: (i) the accuracy of SPPs in detecting long-term urban precipitation trends and (ii) whether comparing two datasets enhances confidence in specific rainfall characteristics.

The precipitation measured by the two datasets correlates poorly (0.35 and 0.46, respectively, for CHIRPS and TAMSAT) with the daily data from the station. This aligns with other studies [23,24,40] that found low correlation values between SPPs and daily station data for Burkina Faso. However, another study of the Sahelian zone of Burkina Faso [16], conducted with the two SPPs we used, observed a stronger Pearson correlation and lower False Alarm Rate values. This low daily accuracy may be attributed to the coarse spatial resolution of the satellite products, as well as challenges posed by the semi-arid climate and limited data availability of ground station data for validation. As our research confirms, using coarser spatial and temporal resolutions reduces the accuracy of satellite datasets [41].

The assessment of the SPPs' accuracy at a monthly scale identified a strong monthly correlation (0.99 for both models). Based on aggregated monthly precipitation values, CHIRPS and TAMSAT may be considered reliable tools for detecting seasonal precipitation trends. These findings agree with other studies [16,23,24].

Overall, due to the better values of Pearson's coefficient, RMSE, and POD, the TAMSAT model performs slightly better than CHIRPS on a daily scale over the area under investigation. Nevertheless, both models could improve on the various daily accuracy statistics.

Regarding the second research question, the two datasets agree on specific precipitation characteristics identified by the ten ETCCDI precipitation indices with the annual cumulation and rainfall intensity increase in some towns. The results are in line with previous studies that found increases in rainfall intensity parameters and cumulative amounts in the Sahel [20,42–44] and Nakanbe-Wayen [18] and Dano [19] catchments in Burkina Faso. The two datasets agree on changes affecting the central portion of the catchment at Bogandé, Manni, and Yalgho towns. The strongly local character of the detected modifications also aligns with the more general changes in the Sahelian rainfall regime, which show strong spatial variability [45] connected to the increase in mesoscale convective systems [46].

The trend comparisons represent a novel approach to urban flood risk assessment, providing a more robust method for detecting precipitation trends in semi-arid areas. This novel approach represents a critical advancement in flood risk assessment methodologies where ground-based data is scarce.

The deviations between the two models concern indices of the duration of precipitation events. Consecutive dry days are increasing in CHIRPS and decreasing on TAMSAT. Consecutive wet days show a slight decrease in CHIRPS, contradicted by stationary trends on TAMSAT. Furthermore, the simple daily intensity index shows a slightly positive trend in the CHIRPS dataset and a stationary or somewhat negative trend in the TAMSAT dataset.

These deviations may be due to the scarcity of data from stations, which, as pointed out by [26], increases the differences in trend detection by the different SPPs. Our study finds that the trends of the CDD, CWD, and SDII indices calculated with different datasets produce less consistent results, which is in agreement with other studies [26,47].

The comparison of trends between station data and satellite products at Bogandé shows some agreement in detecting rainfall intensification, particularly for the RX5day index, where both the station and TAMSAT datasets identified significant increasing trends. However, the satellite datasets differ from the station dataset in detecting changes across other precipitation parameters. These discrepancies likely stem from the inherent differences between point measurements from ground stations and gridded satellite estimates and the different algorithms used to process satellite data into daily rainfall estimates.

The study's major limitation is the lack of a weather station in three investigated towns. On the other hand, the datasets available at the other four town stations have gaps that do not allow for elaborating annual precipitation indices using RClimdex software. Consequently, the many missing years in calculating the ETCCDI indices through station-based rainfall series did not allow for a reliable and complete assessment of climate trends. As a result, it was impossible to have a benchmark to attest to the accuracy of the trends processed using satellite datasets. Filling gaps in station data is an option initially considered but soon discarded as automatic data homogenization and filling software (i.e., the RClimatol package) tend not to work well in areas characterized by seasonal climate and with extreme events such as the Sahel. However, future studies could explore using machine learning algorithms to compile and fill the gaps in the available station series, thereby improving the accuracy of the precipitation trend detection in the area and providing a measure of further evaluation of the results obtained here. This could help refine flood risk assessments and enhance the resilience of urban areas.

The theoretical implication of trend comparisons is that reducing the uncertainty inherent in daily-scale SPPs relating to urban settlements is possible. Towns affected by an increase in precipitation due to very wet days, days of heavy and very heavy rainfall, and five-day maximum precipitation need special attention, as these parameters have been found to trigger pluvial floods [48]. The operational implications of the study concern the analysis of the risk of pluvial flooding on a local scale. Results indicate the importance of locally verifying whether the critical rainfall threshold has also changed to levels beyond which flood damage occurs. The increase in rainfall over five days in Manni and Bogandé suggests that cumulative rain on successive days should be considered in the analysis of pluvial flood risk. The increase in extreme rain and days of heavy rainfall may explain the recent pluvial flooding in Bogandé and Manni and the increase in alertness in Gayéri and Yalgho.

5. Conclusions

This study fills a critical knowledge gap in rainfall trends by providing a novel comparative analysis of satellite precipitation products (SPPs) in a semi-arid region where ground-based data are scarce. Although SPPs are used in long-term climate analyses, their accuracy on a daily scale may need improvement and should be tested locally on a case-by-case basis.

This study aimed to (i) investigate the accuracy of two SPPs in reproducing long-term urban rainfall and (ii) to test whether using two SPPs to extract urban rainfall trends can increase confidence in the results.

The performance of the two SPPs revealed low values of the daily statistical indices and excellent correlation on the monthly scale. Moreover, the two SPPs agreed on some precipitation trends in individual towns, thus making it possible to identify significant changes with more confidence.

The first novelty of the study is the comparison between rainfall trends in urban settlements obtained from two datasets. The second novelty is characterizing changes in urban rainfall in a large catchment (39,138 km^2) that has been severely flooded in recent years but still needs better investigation. The indices applied to the two datasets agree to show an increase in cumulative annual precipitation and several significant and positive trends in precipitation intensity over some of the investigated towns.

These findings emphasize the urgent need for pluvial flood prevention strategies, especially in Bogandé and Manni, where increasing trends in heavy rainfall raise risks. Policymakers can use these data to inform future infrastructure development and improve urban resilience to flooding.

Future research could explore integrating additional satellite datasets and employing machine learning techniques to fill gaps in ground data and refine the accuracy of rainfall trend detection.

This study's comparative approach improves the characterization of rainfall trends, offering a replicable model for urban settlements facing similar data limitations.

Author Contributions: Conceptualization, G.C. and A.P.; methodology, A.P., software, G.C.; data collection, G.C. and M.T.; article structuring, A.P. and M.T.; writing—first draft, G.C.; writing—review, A.P. and M.T.; fund search, M.T. All authors have read and agreed to the published version of the manuscript.

Funding: This research received no external funding.

Data Availability Statement: The RClimdex software is available at: https://etccdi.pacificclimate.org/software.shtml, accessed on 10 April 2024. The satellite precipitation datasets used in the study and the ETCCDI index computations are available online at: https://data.mendeley.com/datasets/jx5hnnw99d/2, accessed on 17 October 2024.

Acknowledgments: The authors thank Joël Zoungrana, National Meteorological Agency of Burkina Faso, for providing the rainfall data from the 11 active stations in the Sirba catchment. This article was prepared in the framework of the SLAPIS-Sahel project, funded by the Italian Agency for Development Cooperation (AID 012487).

Conflicts of Interest: The authors declare no conflict of interest.

References

1. Herrmann, S.M.; Brandt, M.; Rasmussen, K.; Fensholt, R. Accelerating Land Cover Change in West Africa over Four Decades as Population Pressure Increased. *Commun. Earth Environ.* **2020**, *1*, 53. [CrossRef]
2. Ouattara, Z.A.; Kabo-Bah, A.T.; Dongo, K.; Akpoti, K.; Siabi, E.K.; Kablan, M.K.A.; Kangah, K.M. Operational and Structural Diagnosis of Sewerage and Drainage Networks in Côte d'Ivoire, West Africa. *Front. Sustain. Cities* **2023**, *5*, 1032459. [CrossRef]
3. Fofana, M.; Adounkpe, J.; Larbi, I.; Hounkpe, J.; Djan'na Koubodana, H.; Toure, A.; Bokar, H.; Dotse, S.-Q.; Limantol, A.M. Urban Flash Flood and Extreme Rainfall Events Trend Analysis in Bamako, Mali. *Environ. Chall.* **2022**, *6*, 100449. [CrossRef]
4. Alexander, L.V.; Fowler, H.J.; Bador, M.; Behrangi, A.; Donat, M.G.; Dunn, R.; Funk, C.; Goldie, J.; Lewis, E.; Rogé, M.; et al. On the Use of Indices to Study Extreme Precipitation on Sub-Daily and Daily Timescales. *Environ. Res. Lett.* **2019**, *14*, 125008. [CrossRef]
5. Klein Tank, A.M.G.; Zwiers, F.W.; Zhang, X. *Guidelines on Analysis of Extremes in a Changing Climate in Support of Informed Decisions for Adaptation*; World Meteorological Organization: Geneva, Switzerland, 2009.
6. Dietzsch, F.; Andersson, A.; Ziese, M.; Schröder, M.; Raykova, K.; Schamm, K.; Becker, A. A Global ETCCDI-Based Precipitation Climatology from Satellite and Rain Gauge Measurements. *Climate* **2017**, *5*, 9. [CrossRef]
7. Chervenkov, H.; Slavov, K. ETCCDI Climate Indices for Assessment of the Recent Climate over Southeast Europe. In *Advances in High Performance Computing*; Dimov, I., Fidanova, S., Eds.; Studies in Computational Intelligence; Springer International Publishing: Cham, Switzerland, 2021; Volume 902, pp. 398–412. ISBN 978-3-030-55346-3.
8. Bewket, W.; Tibebe, D.; Teferi, E.; Degefu, M.A. Changes in Mean and Extreme Rainfall Indices over a Problemscape in Central Ethiopia. *Environ. Chall.* **2024**, *15*, 100883. [CrossRef]
9. Levizzani, V.; Cattani, E. Satellite Remote Sensing of Precipitation and the Terrestrial Water Cycle in a Changing Climate. *Remote Sens.* **2019**, *11*, 2301. [CrossRef]
10. Sanogo, S.; Peyrillé, P.; Roehrig, R.; Guichard, F.; Ouedraogo, O. Extreme Precipitating Events in Satellite and Rain Gauge Products over the Sahel. *J. Clim.* **2022**, *35*, 1915–1938. [CrossRef]
11. Keikhosravi-Kiany, M.S.; Masoodian, S.A.; Balling Jr, R.C. Reliability of Satellite-Based Precipitation Products in Capturing Extreme Precipitation Indices over Iran. *Adv. Space Res.* **2023**, *71*, 1451–1472. [CrossRef]
12. Petković, V.; Brown, P.J.; Berg, W.; Randel, D.L.; Jones, S.R.; Kummerow, C.D. Can We Estimate the Uncertainty Level of Satellite Long-Term Precipitation Records? *J. Appl. Meteorol. Climatol.* **2023**, *62*, 1069–1082. [CrossRef]
13. Maggioni, V.; Massari, C.; Kidd, C. Errors and Uncertainties Associated with Quasiglobal Satellite Precipitation Products. In *Precipitation Science*; Elsevier: Amsterdam, The Netherlands, 2022; pp. 377–390. ISBN 978-0-12-822973-6.
14. Maggioni, V.; Meyers, P.C.; Robinson, M.D. A Review of Merged High-Resolution Satellite Precipitation Product Accuracy During the Tropical Rainfall Measuring Mission (TRMM) Era. *J. Hydrometeorol.* **2016**, *17*, 1101–1117. [CrossRef]
15. Gebremichael, M.; Bitew, M.M.; Hirpa, F.A.; Tesfay, G.N. Accuracy of Satellite Rainfall Estimates in the Blue Nile Basin: Lowland Plain Versus Highland Mountain. *Water Resour. Res.* **2014**, *50*, 8775–8790. [CrossRef]
16. Garba, J.N.; Diasso, U.J.; Waongo, M.; Sawadogo, W.; Daho, T. Performance Evaluation of Satellite-Based Rainfall Estimation Across Climatic Zones in Burkina Faso. *Theor. Appl. Climatol.* **2023**, *154*, 1051–1073. [CrossRef]
17. Zhou, L.; Koike, T.; Takeuchi, K.; Rasmy, M.; Onuma, K.; Ito, H.; Selvarajah, H.; Liu, L.; Li, X.; Ao, T. A Study on Availability of Ground Observations and Its Impacts on Bias Correction of Satellite Precipitation Products and Hydrologic Simulation Efficiency. *J. Hydrol.* **2022**, *610*, 127595. [CrossRef]
18. Yameogo, W.V.M.; Akpa, Y.L.; Danumah, J.H.; Traore, F.; Tankoano, B.; Sanon, Z.; Kabore, O.; Hien, M. Spatio-Temporal Evolution of Rainfall over the Period 1981–2020 and Management of Surface Water Resources in the Nakanbe–Wayen Watershed in Burkina Faso. *Earth* **2023**, *4*, 606–626. [CrossRef]

19. Okafor, G.C.; Larbi, I.; Chukwuma, E.C.; Nyamekye, C.; Limantol, A.M.; Dotse, S.-Q. Local Climate Change Signals and Changes in Climate Extremes in a Typical Sahel Catchment: The Case of Dano Catchment, Burkina Faso. *Environ. Chall.* **2021**, *5*, 100285. [CrossRef]
20. Sacré Regis M., D.; Mouhamed, L.; Kouakou, K.; Adeline, B.; Arona, D.; Houebagnon Saint. J., C.; Koffi Claude A., K.; Talnan Jean H., C.; Salomon, O.; Issiaka, S. Using the CHIRPS Dataset to Investigate Historical Changes in Precipitation Extremes in West Africa. *Climate* **2020**, *8*, 84. [CrossRef]
21. Bichet, A.; Diedhiou, A. West African Sahel Has Become Wetter During the Last 30 Years, but Dry Spells Are Shorter and More Frequent. *Clim. Res.* **2018**, *75*, 155–162. [CrossRef]
22. Atiah, W.A.; Mengistu Tsidu, G.; Amekudzi, L.K.; Yorke, C. Trends and Interannual Variability of Extreme Rainfall Indices over Ghana, West Africa. *Theor. Appl. Climatol.* **2020**, *140*, 1393–1407. [CrossRef]
23. Dembélé, M.; Zwart, S.J. Evaluation and Comparison of Satellite-Based Rainfall Products in Burkina Faso, West Africa. *Int. J. Remote Sens.* **2016**, *37*, 3995–4014. [CrossRef]
24. Satgé, F.; Defrance, D.; Sultan, B.; Bonnet, M.-P.; Seyler, F.; Rouché, N.; Pierron, F.; Paturel, J.-E. Evaluation of 23 Gridded Precipitation Datasets Across West Africa. *J. Hydrol.* **2020**, *581*, 124412. [CrossRef]
25. Goudiaby, O.; Bodian, A.; Dezetter, A.; Diouf, I.; Ogilvie, A. Evaluation of Gridded Rainfall Products in Three West African Basins. *Hydrology* **2024**, *11*, 75. [CrossRef]
26. Alexander, L.V.; Bador, M.; Roca, R.; Contractor, S.; Donat, M.G.; Nguyen, P.L. Intercomparison of Annual Precipitation Indices and Extremes over Global Land Areas from In Situ, Space-Based and Reanalysis Products. *Environ. Res. Lett.* **2020**, *15*, 055002. [CrossRef]
27. Cattani, E.; Merino, A.; Guijarro, J.A.; Levizzani, V. East Africa Rainfall Trends and Variability 1983–2015 Using Three Long-Term Satellite Products. *Remote Sens.* **2018**, *10*, 931. [CrossRef]
28. Agence Nationale de la Météorologie; World Meteorological Organization Atelier National de Collecte d'Information et de Cartographie Des Sites d'Inondation Au Burkina Faso. *Etude de la Connaissance du Risque D'inondation au Burkina Faso et Choix des Sites Prioritaires Pour l'Alerte Précoce*; Renforcement des Services Hydrométéorologiques pour la Prévision des Crues et Inondations au Burkina Faso; Secrétariat Exécutif du Partenariat Régional de l'Eau de l'Afrique de l'Ouest: Ouagadougou, Burkina Faso.
29. Beck, H.E.; Zimmermann, N.E.; McVicar, T.R.; Vergopolan, N.; Berg, A.; Wood, E.F. Present and Future Köppen-Geiger Climate Classification Maps at 1-Km Resolution. *Sci. Data* **2018**, *5*, 180214. [CrossRef]
30. Aich, V.; Liersch, S.; Vetter, T.; Andersson, J.; Müller, E.; Hattermann, F. Climate or Land Use?—Attribution of Changes in River Flooding in the Sahel Zone. *Water* **2015**, *7*, 2796–2820. [CrossRef]
31. Massazza, G.; Bacci, M.; Descroix, L.; Ibrahim, M.H.; Fiorillo, E.; Katiellou, G.L.; Panthou, G.; Pezzoli, A.; Rosso, M.; Sauzedde, E.; et al. Recent Changes in Hydroclimatic Patterns over Medium Niger River Basins at the Origin of the 2020 Flood in Niamey (Niger). *Water* **2021**, *13*, 1659. [CrossRef]
32. INSD-Institut National de la Statistique et de la Démographie Résultats Cinquième Recensement Général de La Population et de l'Habitation. *Monographie de La Région de l'Est*; INSD: Ouagadougou, Burkina Faso, 2022.
33. INSD-Institut National de la Statistique et de la Démographie Résultats Cinquième Recensement Général de La Population et de l'Habitation. *Monographie de La Région Du Sahel*; INSD: Ouagadougou, Burkina Faso, 2022.
34. Funk, C.; Peterson, P.; Landsfeld, M.; Pedreros, D.; Verdin, J.; Shukla, S.; Husak, G.; Rowland, J.; Harrison, L.; Hoell, A.; et al. The Climate Hazards Infrared Precipitation with Stations—A New Environmental Record for Monitoring Extremes. *Sci. Data* **2015**, *2*, 150066. [CrossRef]
35. Du, H.; Tan, M.L.; Zhang, F.; Chun, K.P.; Li, L.; Kabir, M.H. Evaluating the Effectiveness of CHIRPS Data for Hydroclimatic Studies. *Theor. Appl. Climatol.* **2024**, *155*, 1519–1539. [CrossRef]
36. Maidment, R.I.; Grimes, D.; Allan, R.P.; Tarnavsky, E.; Stringer, M.; Hewison, T.; Roebeling, R.; Black, E. The 30 Year TAMSAT African Rainfall Climatology and Time Series (TARCAT) Data Set. *J. Geophys. Res. Atmos.* **2014**, *119*, 10619–10644. [CrossRef]
37. Maidment, R.I.; Grimes, D.; Black, E.; Tarnavsky, E.; Young, M.; Greatrex, H.; Allan, R.P.; Stein, T.; Nkonde, E.; Senkunda, S.; et al. A New, Long-Term Daily Satellite-Based Rainfall Dataset for Operational Monitoring in Africa. *Sci. Data* **2017**, *4*, 170063. [CrossRef] [PubMed]
38. Sen, P.K. Estimates of the Regression Coefficient Based on Kendall's Tau. *J. Am. Stat. Assoc.* **1968**, *63*, 1379–1389. [CrossRef]
39. Mann, H.B. Nonparametric Tests Against Trend. *Econometrica* **1945**, *13*, 245–259. [CrossRef]
40. Yonaba, R.; Belemtougri, A.; Fowé, T.; Mounirou, L.A.; Nkiaka, E.; Dembélé, M.; Komlavi, A.; Coly, S.M.; Koïta, M.; Karambiri, H. Rainfall Estimation in the West African Sahel: Comparison and Cross-Validation of Top-down vs. Bottom-up Precipitation Products in Burkina Faso. *Geocarto Int.* **2024**, *39*, 2391956. [CrossRef]
41. Le Coz, C.; Van De Giesen, N. Comparison of Rainfall Products over Sub-Saharan Africa. *J. Hydrometeorol.* **2020**, *21*, 553–596. [CrossRef]
42. Odoulami, R.C.; Akinsanola, A.A. Recent Assessment of West African Summer Monsoon Daily Rainfall Trends. *Weather* **2018**, *73*, 283–287. [CrossRef]
43. Sanogo, S.; Fink, A.H.; Omotosho, J.A.; Ba, A.; Redl, R.; Ermert, V. Spatio-Temporal Characteristics of the Recent Rainfall Recovery in West Africa. *Int. J. Climatol.* **2015**, *35*, 4589–4605. [CrossRef]
44. Nouaceur, Z.; Murarescu, O. Rainfall Variability and Trend Analysis of Rainfall in West Africa (Senegal, Mauritania, Burkina Faso). *Water* **2020**, *12*, 1754. [CrossRef]

45. Biasutti, M. Rainfall Trends in the African Sahel: Characteristics, Processes, and Causes. *WIREs Clim. Change* **2019**, *10*, e591. [CrossRef]
46. Fitzpatrick, R.G.J.; Parker, D.J.; Marsham, J.H.; Rowell, D.P.; Guichard, F.M.; Taylor, C.M.; Cook, K.H.; Vizy, E.K.; Jackson, L.S.; Finney, D.; et al. What Drives the Intensification of Mesoscale Convective Systems over the West African Sahel Under Climate Change? *J. Clim.* **2020**, *33*, 3151–3172. [CrossRef]
47. Harrison, L.; Funk, C.; Peterson, P. Identifying Changing Precipitation Extremes in Sub-Saharan Africa with Gauge and Satellite Products. *Environ. Res. Lett.* **2019**, *14*, 085007. [CrossRef]
48. Tazen, F.; Diarra, A.; Kabore, R.F.W.; Ibrahim, B.; Bologo/Traoré, M.; Traoré, K.; Karambiri, H. Trends in Flood Events and Their Relationship to Extreme Rainfall in an Urban Area of Sahelian West Africa: The Case Study of Ouagadougou, Burkina Faso. *J. Flood Risk Manag.* **2019**, *12*, e12507. [CrossRef]